Horste et al., Figure S1

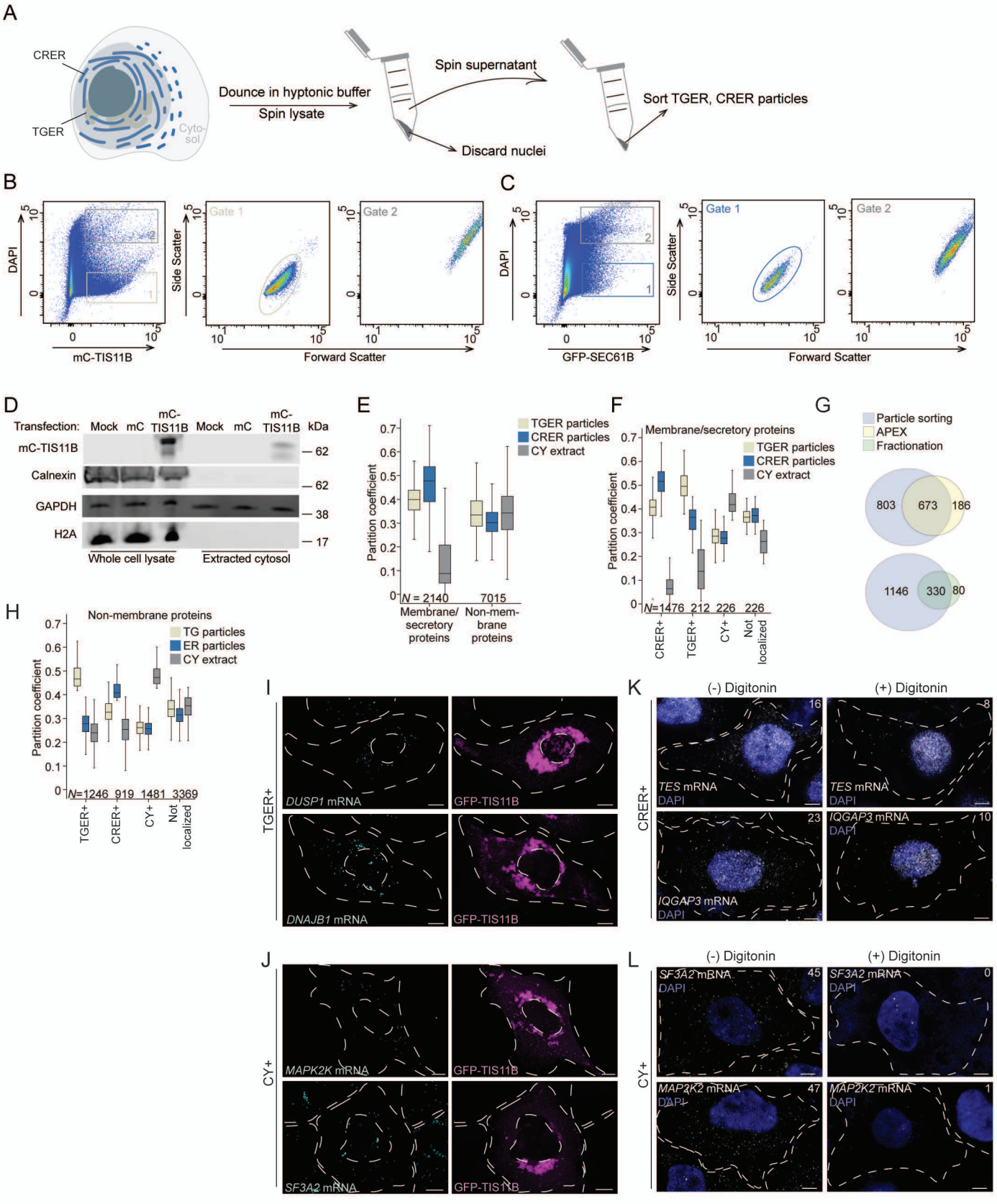

Figure S1. Strategy to determine subcytoplasmic mRNA localization.
(A) Cell fractionation strategy to obtain the cytoplasmic membrane fraction. Transfected HEK293T cells were lysed in hypotonic buffer, followed by douncing and differential centrifugation with 7000 g. The supernatant contains the cytoplasmic membrane fraction that was used for subsequent fluorescent particle sorting.
(B) FACS plot showing mCherry-TIS11B-positive TGER particles costained with DAPI to segregate TGER particles from nuclear contamination. Gate (1) contains TGER particles, whereas gate (2) contains TGER particles bound to nuclei, indicated by DAPI stain and larger size.
(C) As in (B) but shown are GFP-SEC61B-positive CRER particles costained with DAPI. Gate (1) contains CRER particles, whereas gate (2) contains CRER particles bound to nuclei, indicated by DAPI stain and larger size.
(D) Immunoblot showing markers used to evaluate the quality of the digitonin-based cytosol extraction. H2A antibody was used as marker for nuclear components, Calnexin was used as ER marker and GAPDH was used as cytosolic protein. Unassembled TIS11B was observed in the cytosol after transfection with mCherry-tagged TIS11B. Marker expression in whole cell lysates serves as control. mC, mCherry.
(E) Baseline distribution of partition coefficients across the three investigated cytoplasmic compartments is shown separately for mRNAs that encode membrane/secretory proteins and mRNAs that encode non-membrane proteins.
(F) Distribution of partition coefficients in each fractionation sample for compartment-enriched mRNAs that encode membrane/secretory proteins.
(G) Overlap of CRER-enriched mRNAs that encode membrane/secretory proteins (N = 1476) with previous datasets that used alternative isolation methods. APEX-seq, X2 =127, $P < 0.0001$ Fractionation dataset, X2 = 803, $P < 0.0001$.
(H) Distribution of partition coefficients in each fractionation sample for compartment-enriched mRNAs that encode non-membrane proteins.
(I) smRNA-FISH of endogenous mRNAs (teal), predicted to localize to the TGER in HeLa cells. The TGER domain is visualized by GFP-TIS11B (magenta). Cell and nuclear boundaries are indicated by the dotted lines. Representative images are shown. Scale bar, 5 µm. Shown are representative images for *DUSP1* and *DNAJB1*.
(J) As in (I), but for endogenous mRNAs predicted to localize to the cytosol in HeLa cells. Shown are representative images for *MAP2K2* and *SF3A2*.
(K) smRNA-FISH of endogenous mRNAs predicted to localize to the CRER. Shown are HeLa cells before (-) and after (+) digitonin treatment. Cell and nuclear boundaries are indicated by the dotted lines, number of foci counted in each image indicated in white. Representative images for *TES* and *IQGAP3* are shown. Scale bar, 5 µm.
(L) As in (K), but for endogenous mRNAs predicted to localize to the cytosol in HeLa cells. Shown are representative images for *SF3A2* and *MAP2K2*.

Horste et al., Figure S2

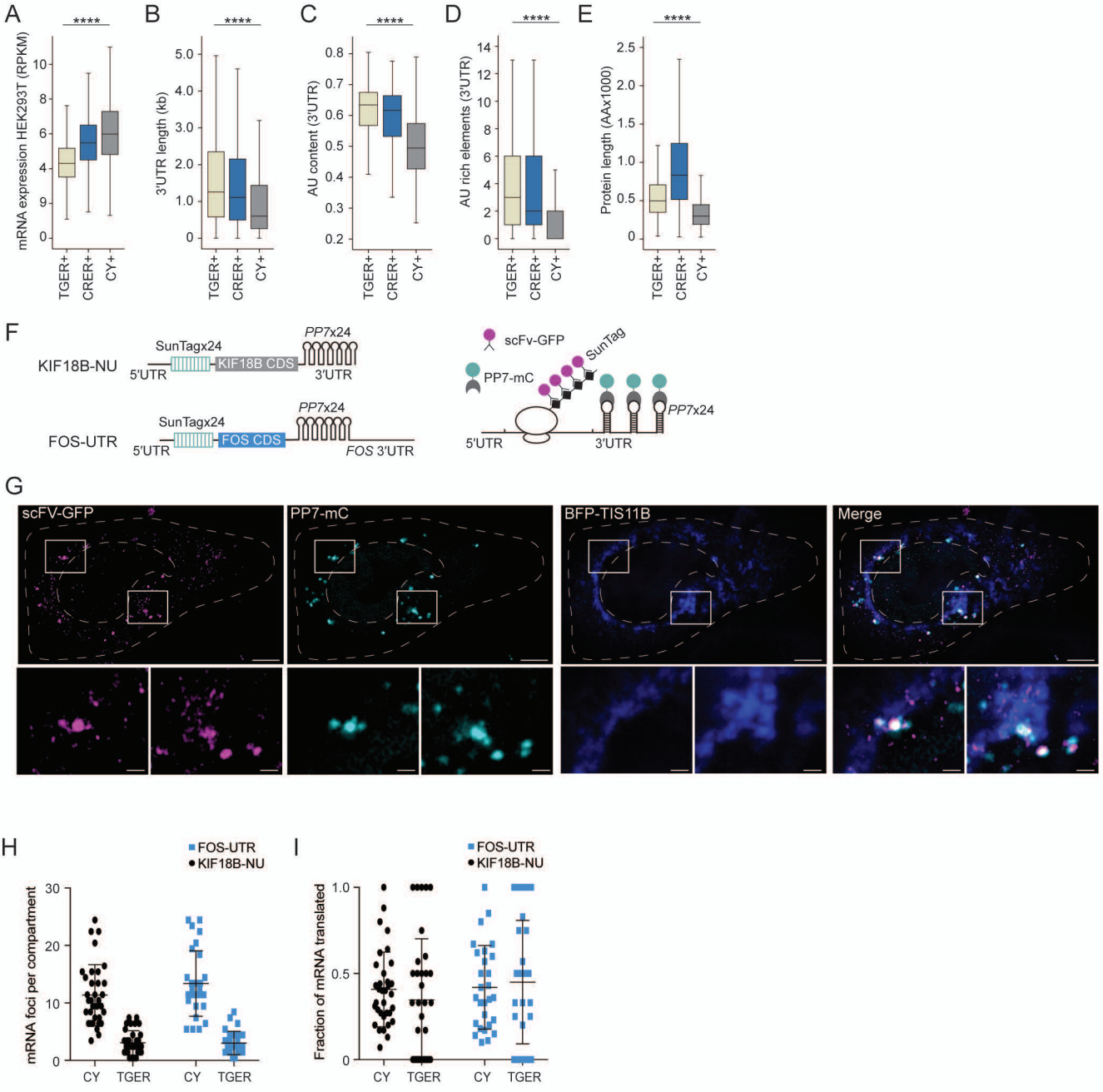

Figure S2. The TGER domain is an active translation compartment.
(A) As in Fig. 2C, but steady-state mRNA abundance levels of compartment-enriched mRNAs obtained by RNA-seq from whole cell lysates of HEK293 cells. This sample was used together with the Pro-seq sample to estimate mRNA half-lives. Kruskal-Wallis test: ****, P = 8 E-146.
(B) As in Fig. 2A, but 3′UTR length of mRNAs enriched in the indicated compartments is shown. Kruskal-Wallis test: ****, P = 4 E-56.
(C) As in (B), but the fraction of adenosines or uridines in 3′UTRs of mRNAs enriched in the indicated compartments is shown. Kruskal-Wallis test: ****, P = 6 E-165.
(D) As in (B), but the number of AU-rich elements (AUUUA) in 3′UTRs of mRNAs enriched in the indicated compartments is shown. Kruskal-Wallis test: ****, P = 2 E-131.
(E) As in (B), but size of mRNA-encoded proteins enriched in the indicated compartments is shown. Kruskal-Wallis test: ****, P = 4 E-241.
(F) Schematic of reporter mRNAs used with the SunTag system to measure nascent protein synthesis. CDS, coding sequence, NU, no UTR. The KIF18B construct serves as positive control as it was used previously (Yan et al., 2016). The FOS-UTR construct was used as *FOS* mRNA is enriched in the TGER domain (Table S2).
(G) Confocal imaging of HeLa cells stably expressing SunTag reporter proteins svFc-GFP and mCherry-tagged PP7 protein (mC-PP7) co-transfected with two constructs (i) BFP-TIS11B to visualize the TGER domain and (ii) SunTag-labeled mRNA encoding FOS together with its 3′UTR and PP7-binding sites. The *FOS* mRNA is visualized by mC-PP7 binding (teal) whereas the FOS protein is visualized by svFc-GFP binding (magenta). Foci with co-localization of mRNA and protein represent nascent protein synthesis and are indicative of active translation. A representative example is shown. Scale bar, 5 μm.
(H) Quantification of the experiment from (G). Shown are the number of mRNA foci in TGER or the cytosol (CY) using the two different Suntag reporters from (F). For the KIF18B reporter, N = 24 cells were analyzed and for the FOS reporter N = 28 cells were analyzed. The FOS-UTR construct was expected to be enriched in the TGER domain compared to the cytosol as endogenous *FOS* mRNA (Table S2) and a *FOS* mRNA expressed from a cDNA construct containing the FOS coding sequence together with its 3′UTR (but lacking the SunTag and the PP7 sites) are enriched in the TGER domain (Fig. 4A-C). This suggests that endogenous mRNA localization is not recapitulated with the SunTag reporter, but this system can still be used to examine active translation.
(I) As in (H), but shown are the mRNAs that are actively translated in each compartment, which were identified by counting the teal and magenta-double positive foci.

Horste et al., Figure S3

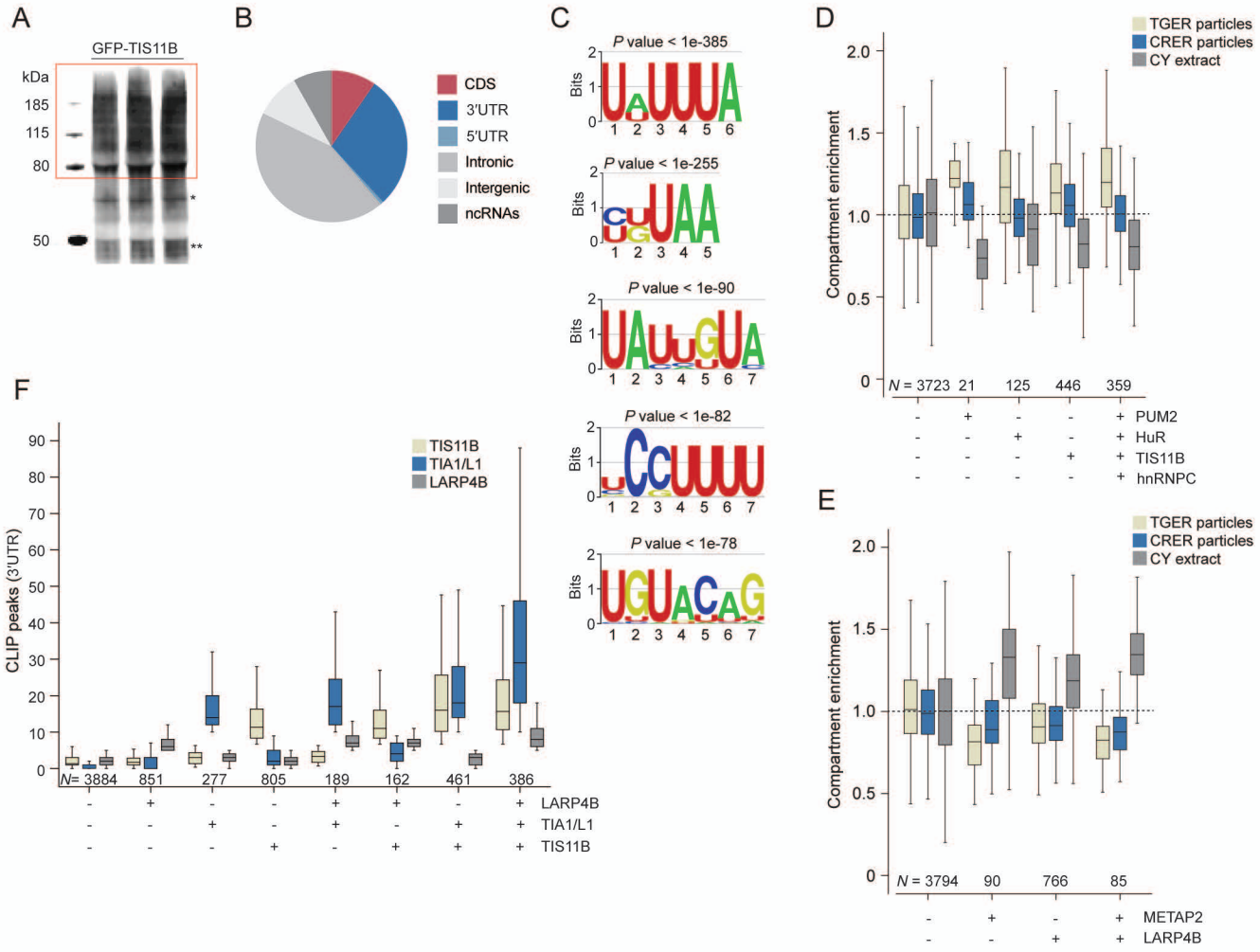

Figure S3. CLIP analysis of RNA-binding proteins.
(A) Gel showing samples used for iCLIP of GFP-tagged TIS11B. The region outlined in red was used for iCLIP sample preparation.
(B) TIS11B iCLIP tag distribution obtained from HEK293T cells.
(C) The top five motifs that were enriched within TIS11B peaks in 3′UTRs compared to all nucleotides in 3′UTRs. Shown are *P* values obtained by HOMER.
(D) Compartment-specific enrichment of mRNAs bound by the indicated AU-rich RNA-binding proteins. Plus (+) indicates the targets of the RNA-binding protein, minus (-) indicates the non-targets. HuR targets have 3′UTRs with more than four HuR peaks, PUM2 targets have 3′UTRs with more than two PUM2 peaks, TIS11B targets have 3′UTRs with more than six TIS11B peaks, HNRNPC targets have 3′UTRs with more than one HNRNPC peak. Mann Whitney tests were performed to investigate enrichment in TGER: (-) vs (+) for PUM2, *P* = 3E-4; (-) vs (+) for HuR, *P* = 2E-7; (-) vs (+) for TIS11B, *P* = 3E-28; (-) vs (+) for all four RNA-binding proteins, *P* = 3E-42.
(E) Compartment-specific enrichment of mRNAs bound by LARP4B, METAP2, or both. Plus (+) indicates the targets of the RNA-binding protein, minus (-) indicates the non-targets. LARP4B targets have 3′UTRs with more than four LARP4B peaks, METAP2 targets have 3′UTRs with more than one METAP2 peak. Mann Whitney tests were performed to investigate enrichment in CY: (-) vs (+) for METAP2, *P* = 3E-16; (-) vs (+) for LARP4B, *P* = 1E-55; (-) vs (+) for both RNA-binding proteins, *P* = 9E-23.
(F) Number of CLIP peaks for the indicated groups of mRNAs. Plus (+) indicates the targets of the specified RNA-binding protein, minus (-) indicates the non-targets.

Horste, et al., Figure S4

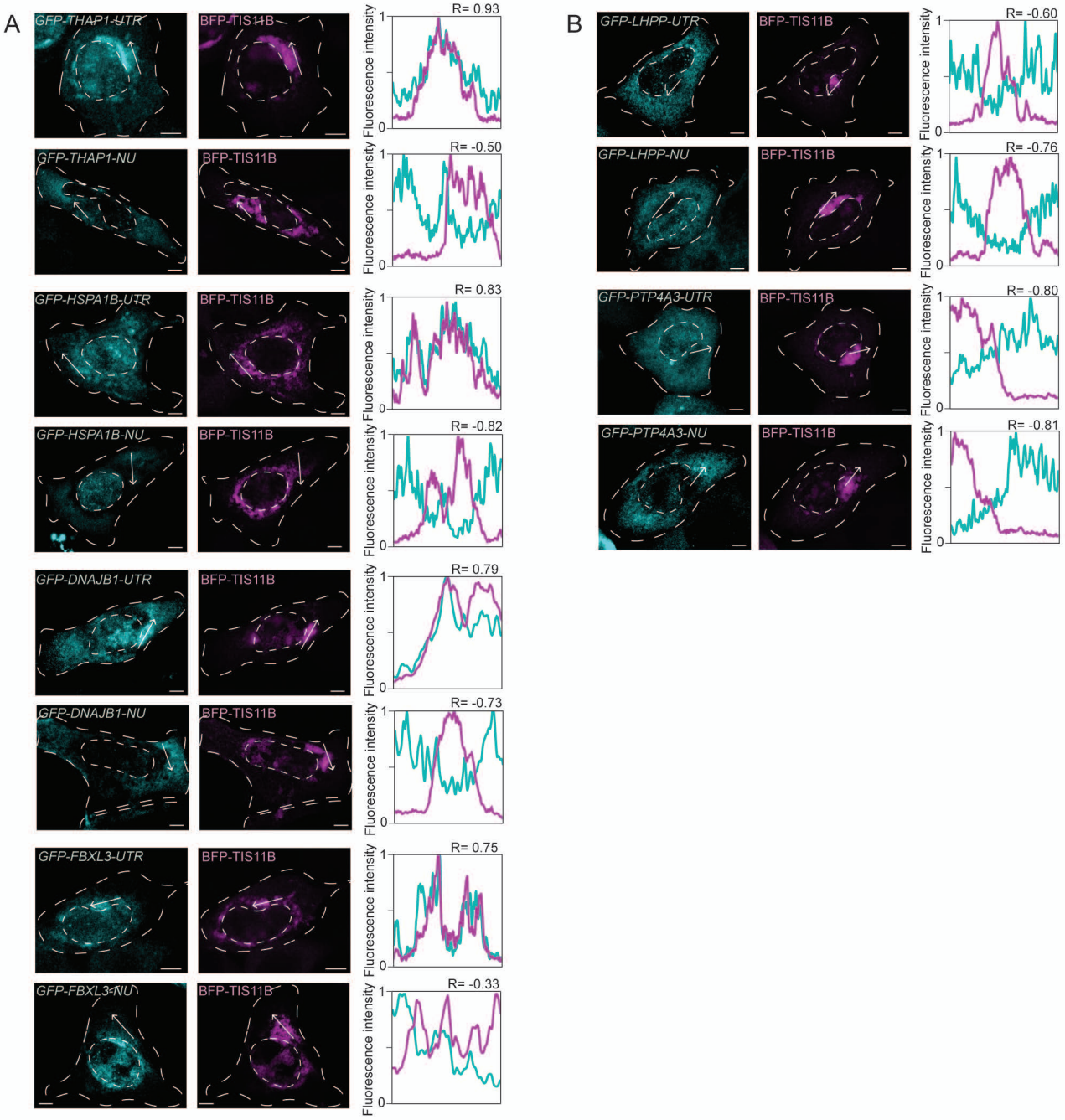

Figure S4. mRNA localization to the TGER domain is controlled by 3′UTRs.
(A) RNA-FISH of mRNAs after transfection of cDNA constructs containing the indicated coding regions, either including (UTR) or excluding the respective 3'UTRs (NU, no UTR) in HeLa cells (teal). GFP-TIS11B was cotransfected to visualize the TGER domain (magenta). Scale bar, 5 µm. Line diagrams showing the fluorescence intensities obtained at the position of the arrows. Shown are representative images for TGER-enriched mRNAs *DNAJB1*, *HSPA1B*, *THAP1*, and *FBXL3*.
(B) As in (A), but for mRNAs predicted to be enriched in the cytosol, *LHPP* and *PTP4A3*.

Horste, et al., Figure S5

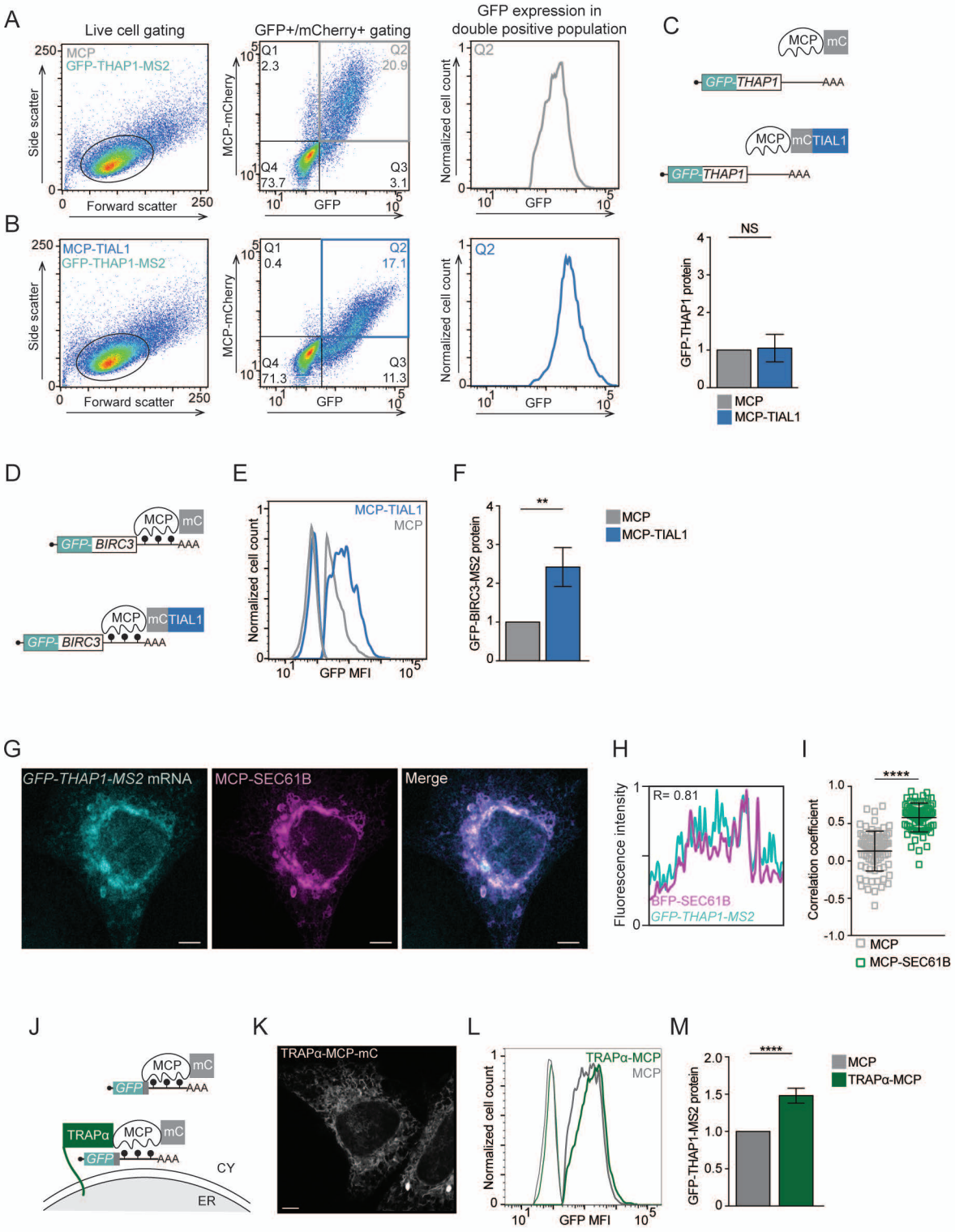

Figure S5. mRNA localization-dependent protein expression of the GFP reporter.
(A) Gating strategy to assess GFP protein expression of the reporter mRNA by FACS. Left panel shows the ungated population of HeLa cells coexpressing MCP-mCherry and the GFP-THAP1-MS2 reporter, separated by size (forward scatter) and granularity (side scatter). The black circle indicates the live cells that were used for subsequent analysis. Middle panel, the GFP- and mCherry-double positive population was gated to obtain the GFP mean fluorescence values (MFI, right panel) which corresponds to the reported GFP protein expression values.
(B) As in (A), but HeLa cells coexpressing MCP-mCherry-TIAL1 and the GFP-THAP1-MS2 reporter.
(C) As in Fig. 4C and 4J, but the MS2 sites in the GFP reporter were omitted. Coexpression of MCP-mCherry-TIAL1 does not result in the binding of MCP to the reporter mRNA. This experiment serves as control for the effect of TIA1L1 overexpression on reporter mRNA expression.
(D) Schematic of a second mRNA reporter used to validate the effect of a single 3′UTR-bound RNA-binding protein on protein expression. The GFP-tagged reporter mRNA contains the BIRC3 coding region and MS2 hairpins as 3′UTR, which allow binding of the co-transfected MS2 coat protein (mCherry-tagged MCP). Fusion of TIAL1 to MCP tethers TIAL1 to the 3′UTR of the reporter mRNA. mC, mCherry.
(E) GFP protein expression of the reporter mRNA from (D) in HeLa cells, coexpressing the indicated MCP-fusion constructs, measured by FACS. Representative histograms are shown. The histograms on the left indicate GFP-negative cell populations.
(F) Quantification of the experiment shown in (E). Shown is the mean ± std of five independent experiments. T-test for independent samples, **, $P = 0.005$.
(G) RNA-FISH of the GFP reporter mRNA (teal) from Fig. 5A in HeLa cells coexpressing MCP-mCherry-SEC61B (magenta) to visualize colocalization between the mRNA and the rough ER membrane. Representative confocal images are shown. Scale bar, 5 µm.
(H) Line profiles of the fluorescence intensities of the arrows from (G).
(I) Quantification of the experiment from (G). Two line profiles were generated for each cell. The Pearson's correlation coefficients of between the reporter mRNA and the ER was determined. For MCP, $N = 26$ cells were analyzed, for MCP-SEC61B, $N = 26$ cells were analyzed. The horizontal line denotes the median and the error bars denote the 25th and 75th percentiles. Mann-Whitney test, ****, $P < 0.0001$.
(J) Schematic of a second GFP-tagged mRNA reporter that investigates the influence of subcellular mRNA localization on protein expression. Fusion of MCP to TRAPα localizes the GFP reporter mRNA to the ER membrane, whereas MCP alone localizes it to the cytosol.
(K) Confocal live cell imaging of HeLa cells expressing mC-tagged TRAPα-MCP. Scale bar, 5 µm.
(L) GFP protein expression of the reporter mRNAs from (J) coexpressing the indicated MCP-fusion constructs in HeLa cells measured by FACS. Representative histograms are shown. The histograms on the left indicate GFP-negative cell populations.
(M) Quantification of the experiment from (L). Shown is the mean ± std of four independent experiments. T-test for independent samples, ****, $P < 0.0001$.

Horste, et al., Figure S6

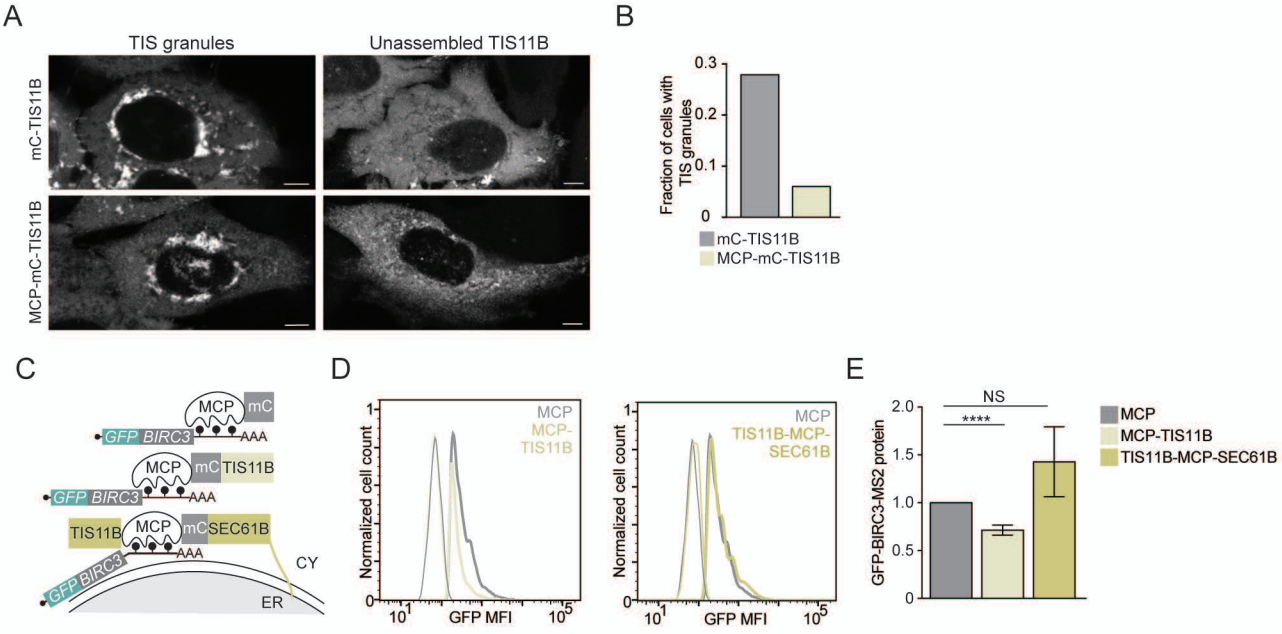

Figure S6. Redirecting mRNA localization from the cytosol to the rough ER overcomes the repressive effect of a bound RNA-binding protein.

(A) Confocal live cell imaging of HeLa cells expressing the indicated constructs. Shown are representative images with TIS granules or unassembled TIS11B. mC, mCherry. Scale bar, 5 µm.

(B) Quantification from (A). The fraction of HeLa cells with TIS granules is shown after transfection of the indicated TIS11B fusion constructs. *N* = 165 cells were analyzed for mCherry-TIS11B and *N* = 198 cells were analyzed for MCP-mCherry-TIS11B. MCP-mCherry-TIS11B largely prevents TIS granule formation.

(C) Schematic of a second TIS11B-bound mRNA reporter that allows investigation of mRNA localization-dependent GFP expression. The coding region of the reporter is provided by BIRC3, followed by MS2 binding sites. Tethering of MCP or TIS11B localizes the mRNA reporter to the cytosol, whereas the MCP-TIS11B-SEC61B fusion localizes the mRNA reporter to the rough ER.

(D) GFP protein expression of the reporter mRNA from (C) in HeLa cells, coexpressing the indicated MCP-fusion constructs, measured by FACS. Representative histograms are shown. The histograms on the left indicate GFP-negative cell populations.

(E) Quantification of the experiment from (D). Shown is the mean ± std of four independent experiments. T-test for independent samples, ****, $P < 0.0001$, MCP vs TIS11B-SEC61B: $P = 0.058$; NS).